Journal of the Chinese Society of Mechanical Engineers, Vol.47, No.1, pp 97~103 (2026)

Analysis of Pedestrian Lower Limb Safety in Pedestrian-SUV Impact and Study of Structural Parameters of Headlights

Sen Xiao*, Li-Dong Zhang*, Chen-Yang Ji*, Bao-Feng Lv**, Yao-Xin He**and Bao-Tian Qu***

Keywords： lower limb injury, pedestrian safety, headlight, SUV, aPLI

ABSTRACT

In a pedestrian–vehicle impact, the lower limbs of pedestrians are extremely vulnerable to injury. In this study, pedestrian lower limb injury was analyzed by establishing the front-end of a sport utility vehicle and advanced pedestrian legform impactor impact conditions. Moreover, a structural parametric study based on the headlight movement space was conducted to reduce pedestrian lower limb injury. Results showed that the maximum bending moment of pedestrians' lower limbs was reduced by 73 Nm when the headlight rearward movement space was increased by 40 mm. Results also indicated that when pedestrians collided with the car headlight, the kinetic energy of their lower limbs was reduced owing to the rearward movement of the headlight. Consequently, injuries suffered by pedestrians' lower limbs were reduced. This study provides a reference for pedestrian lower limb protection.

INTRODUCTION

Pedestrians, as vulnerable road users, are susceptible to serious injuries in traffic accidents. Among all types of traffic accidents, pedestrian–vehicle impact accounts for about 20% of the total accidents, and pedestrian fatalities account for about a quarter of traffic accident deaths (Cheng et al., 2022; Wang et al., 2019). In a pedestrian–vehicle impact, pedestrians' lower limbs are usually the first to collide with the front of the vehicle and are the most vulnerable part of the body in accidents (Cater et al., 2008; Mo et al., 2018). Injuries to the lower limbs of pedestrians resulting from impact with the front-end structures of automobiles are primarily tibia fractures and knee injuries (Aekbote et al., 2003). Although injuries to the lower limbs generally do not result in pedestrian fatalities, such injuries may lead to knee dislocations, ligament tears, and even permanent disability (Altai et al., 2018; Mo et al., 2017). Therefore, pedestrian leg impact safety research remains a non-negligible element.

Advanced pedestrian legform impactor (aPLI) has the advantages of good reliability and high fidelity (Isshiki et al., 2016; Long et al., 2021) and is an important approach for evaluating pedestrian safety. Previous studies have compared the characteristics of aPLI with those of flexible PLI (Flex-PLI). The aPLI is based on the latest bionic design of the human leg, optimizing the shape of the leg and using more advanced biomimetic materials (Chen et al., 2021a). What's more, aPLI not only adds a new simplified mass block, but also its mass distribution is closer to the real human lower limb (Cao et al., 2024, Wei et al., 2021). This enables aPLI to more accurately simulate the degree of damage to the human leg during a collision, thus allowing for a more objective assessment of the vehicle's pedestrian protection performance. Some studies have proposed vehicle improvement programs based on the aPLI impact tests (Hou et al., 2020, Fu et al., 2020). However, research on improving the structural position parameters of headlights to increase pedestrian leg safety is not yet complete.

At present, sport utility vehicle (SUV) SUV sales are gradually increasing and has become the main force of the automobile market growth in recent years. In particular, small and medium-sized SUVs, represented by Great Wall Motor, have a considerably high market share. SUVs usually have a high ground clearance, with the bottom of the body higher above the ground. Compared with passenger

Paper Received April, 2024. Revised May, 2025, Accepted May, 2025, Author for Correspondence:Baotian QU, 147966863@qq.com

* *School of Mechanical Engineering, Hebei University of Technology, Tianjin, 300401, China.*

** *Hebei Automobile Technology Innovation Center, Great Wall Motor Company, Baoding, Hebei, 071000, China.*

*** *Radiology Department of Luodian Hospital, Baoshan District, Shanghai 200400, China.*

cars, the front end of SUVs is more vertical and higher, and the position of bumpers and other structures differs from that of passenger cars (Bhagat et al., 2011). During a collision with a pedestrian, it is more likely to hit the knee or thigh area first. This may cause more serious injuries to the lower limbs and even lead to the death of the pedestrian (Hu et al., 2024, Tyndall., 2024). Some researchers investigated the effect of SUV structure on aPLI and improved the SUV structure to meet the need for pedestrian protection. Hou et al. (2022) investigated the effect of the SUV structure on the crashworthiness of the aPLI and optimized the SUV structure using machine learning. Xu et al. (2021) conducted a simulation impact study of aPLI using an SUV model and gave an improvement strategy for the structure of the light strip area to meet the needs of pedestrian protection. So far, there is a lack of research on optimizing headlight parameters for SUVs to improve pedestrian safety.

This study is based on a certain type of SUV with high market share. According to the test requirements of the China-New Car Assessment Program (C-NCAP) (CATARC., 2024), finite element simulation is used to analyze the injury of aPLI in frontal impact. On the bases of the results of the analysis, the structural parameter of the headlights is investigated to improve the safety of the pedestrian lower limb safety.

MATERIAL AND METHODS

For impact analysis, the correct establishment of the finite element model is an important condition to ensure the reliability of the simulation results.

Research Model

This study focuses on pedestrian leg impact protection. The model used in the study consisted of the aPLI and the vehicle front-end structure (Fig. 1). The vehicle front-end structure was based on one of the SUV models of Great Wall Motor which had a high selling in the market. Components such as the hood assembly, wing, front bumper, headlight, hood, and body-in-white parts were included. The whole model contained a total of 374243 shell elements, 8697 solid elements, and some 1D connection elements. In addition, the full model included a total of 1203904 nodes. Among the materials used in the collision part of the vehicle were PP+EPDM-TD20, ABS plastic, and HC820-1180DP. Automatic face-to-face contact between the vehicle and the aPLI was used, and the coefficient of friction at the contact location was set to 0.3. The front-end structure of the vehicle was immobilized in six degrees of freedom at the A-pillar as well as at the rear end of the floor. Impact the aPLI at 40 km/h on the front-end structure of the vehicle.

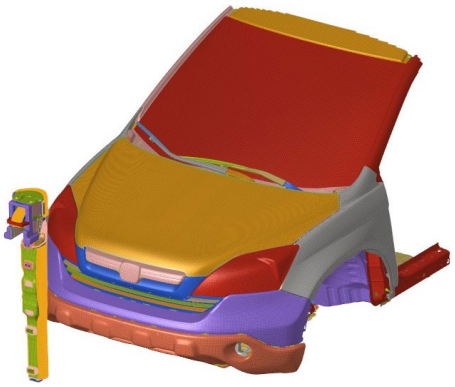

Fig. 1. Pedestrian lower limb impact research model.

APLI Model

The aPLI consisted of skin, muscle, thigh, calf, knee, and simplified upper body part (SUBP) (Chen et al., 2021b). In terms of external dimensions in the front view direction, SUBP had a width of 200±2 mm at the top, width of 142±2 mm at the bottom, and height of 222±2 mm. In the side view of the aPLI model, the thigh and calf cross-sections decreased in size from top to bottom, and the thigh cross-sectional dimensions were larger than those of the calf cross-sectional dimensions. The centers of mass of the thigh, calf, and knee were located 875±10, 205±5, and 495±5 mm, respectively, up from the bottom of the leg. The center of mass of the upper body module was located 961±10 mm above the bottom of the leg. The aPLI leg had a center of mass located 780±10 mm above the bottom of the leg. The upper body module had a moment of inertia of 0.0850±0.004 $kg \cdot m^2$ through its center of mass. The thigh bending moments were measured at Femur_up, Femur_mid, and Femur_low. The calf bending moments were measured at Tibia_up, Tibia_mid_up, Tibia_mid_low, and Tibia_low. The medial collateral ligament (MCL) extension was measured at MCL (Fig. 2).

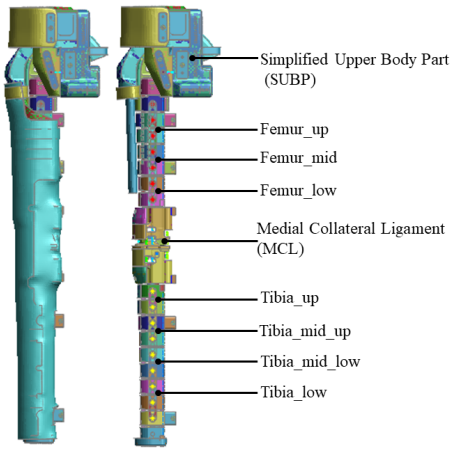

Fig. 2. Basic structure of aPLI.

Impact Point Marker

The network grid points were marked against

the leg test area, starting at the center of the upper bumper reference line, noted as L0. Measurements were taken horizontally in the longitudinal center plane of the vehicle to each side of the vehicle, marking every 100 mm up to the outermost part of the bumper. The locations, which were 600-mm apart from L0, were defined as L+6 and L-6 (Fig. 3).

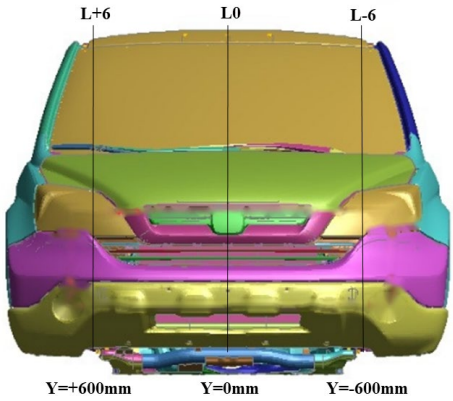

Fig. 3. Schematic of the lower limb impact point marking.

Model Credibility Validation

To ensure the validity of the proposed model, model credibility needs to be calibrated. Given the lack of an external force applied during the entire collision, changes in the total, kinetic, internal, slip, and hourglass energies of the model during the collision should comply with the law of conservation of energy.

Although the location of the impact during the test was not the same, the vehicle model, aPLI model and parameter settings were the same. Therefore, one of the impact points was selected for energy analysis. In this study, the central point of the vehicle leg test area (i.e., L0 position) was selected for analysis (Fig. 4). According to the energy change curve over time the total energy remained constant throughout the process, in accordance with the law of conservation of energy. The kinetic energy of the system was gradually converted to internal energy with time. It stabilized after 40 ms and the energy curve was smooth and level. The highest value of hourglass energy in the study was only 0.95% of the total energy, which was less than 5% of the total energy. The results met the requirement (Matsui et al., 2013). In conclusion, it could be seen that the simulation results of this model were credible.

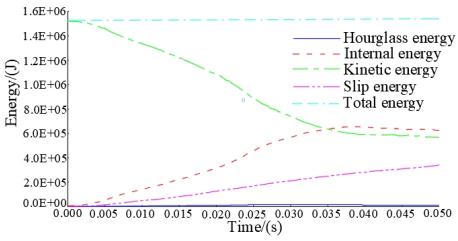

Fig. 4. Energy change curve.

RESULTS

The most marginal positions were L+6 and L-6. Owing to the symmetry of the vehicle's left and right results, only the L+6 position was simulated for impact in this study. Pedestrian leg safety was analyzed according to the C-NCAP requirements. Eight indicators, such as thigh bending moment, calf bending moment, and medial collateral ligament (MCL) extension of the knee, were collected for evaluation during the impact.

Three evaluation indicators for the pedestrian thigh were extracted (Fig. 5). The results showed that the Femur_up bending moment was 416 Nm, which was between the high and low performance limits stipulated by C-NCAP. In addition, the linear interpolation method was used to obtain the corresponding score of 1.04. The Femur_mid bending moment was 455 Nm, which was higher than the low performance limit, and scored 0. The Femur_low bending moment was 389 Nm, which was lower than the high performance limit, and scored 2. The lowest score, 0, was selected for the comprehensive evaluation scores of the model's pedestrian thigh.

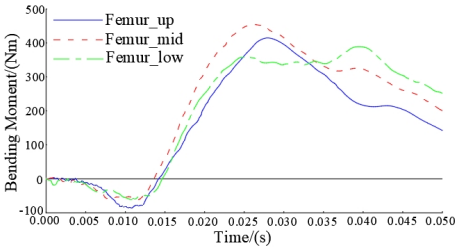

Fig. 5. Thigh bending moment curve.

Analysis of the cause indicated that during the impact, Femur_up touched the headlight, Femur_mid touched the intersection of the headlight and the front bumper, and Femur_low touched the front bumper (Fig. 6). The first peak was generated at this point. Since the material of the headlight was PP+EPDM-TD20, the stiffness was large and the deformation energy absorption was poor. When Femur_up collided with the headlight, the residual velocity was larger, which made the bending moment larger. Femur_mid impact appeared at the same moment as Femur_up, but the reason for the maximum bending moment appeared was different from Femur_up. The main reason for this was the difference in the materials used for the impacts at Femur_up and Femur_low, where the material stiffness was lower and the energy absorption effect was better than that of Femur_up. The difference in velocity between Femur_up and Femur_low at this point was larger, which resulted in a larger bending moment at the Femur_mid. The value of this bending moment exceeded the relevant requirements of C-NCAP.

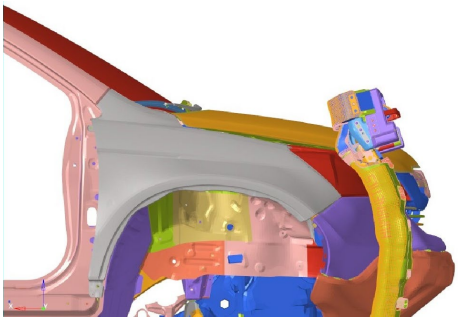

Fig. 6. Lower limb impact diagram.

Evaluation of the results showed that the model's base state aPLI thigh safety evaluation did not meet the C-NCAP score target.

Extraction of four indicators of safety evaluation of the pedestrian calf (Fig. 7). Tibia_up, Tibia_mid_up, Tibia_mid_low, and Tibia_low were 142, 126, 97, and 45 Nm, respectively, which were lower than the high-performance limit values. Therefore, the score of the calf evaluation was 2.

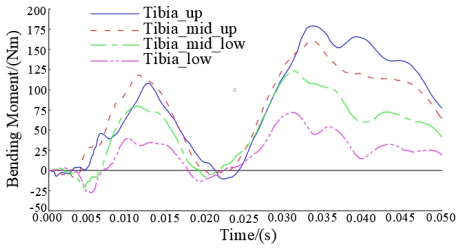

Fig. 7. Calf bending moment curve.

Analysis showed that the first peak of the calf bending moment occurred between 10 ms and 15 ms. At this time, the knee part stopped moving forward by colliding with the front bumper. However, only a significantly small portion of the calf part had a direct impact with the car, while the rest of the part continued to move forward. Consequently, this process generated torque owing to the presence of a velocity difference. Tibia_up and Tibia_mid_up were resisted by collision with the front bumper, so the bending moment was substantial at these points. The second crest occurred between 30 ms and 35 ms. The reason for this was that the calf started to rebound at the end of the impact, thereby gaining reverse velocity. Furthermore, the bending moment reached its maximum value.

The amount of ligament extension can reflect the degree of injury (You et al., 2003). The maximum value of MCL of ligament extension, the only indicator for knee evaluation, was 14.3 mm (Fig. 8). This value was below the high-performance limit specified by C-NCAP, so the knee evaluation score was 1.

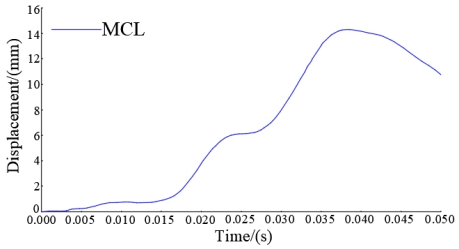

Fig. 8. Knee ligament extension curve.

Analysis showed that the ligament elongation continued to increase from the beginning of the collision to 37.5 ms. After reaching a maximum value of 14.3 mm, the ligament elongation decreased. During impact, the knee collided with the bumper part of the car. Owing to the high stiffness of the bumper, the knee stopped moving, while the thigh and calf parts continued to move forward. Thus, ligament elongation increased from 0 ms to 37.5 ms. Meanwhile, ligament elongation began to decrease in the posterior portion of the segment owing to the completion of the impact when the thigh and calf began to rebound backward.

The final safety score for the lower limbs of pedestrians in the impact case of this model was 3 (Table 1) based on C-NCAP's comprehensive analysis of the safety scores for each part of the legs. The reason was that the calf bending moment and knee ligament elongation complied with the C-NCAP requirements. Meanwhile, the bending moment at the thigh was higher than the performance limit, resulting in a low score at the headlight.

Table 1. Sheet of the Dummy Score.

Parameters	Performance limits	Injury values	Scores	
Femur_up	390–440 Nm	416 Nm	1.04	
Femur_mid		455 Nm	0	0
Femur_low		389 Nm	2	
MCL	27–32 mm	14.3 mm	1	1
Tibia_up	275–320 Nm	142 Nm	2	2
Tibia_mid_up		126 Nm	2	
Tibia_mid_low		97 Nm	2	
Tibia_low		45 Nm	2	
Total score			3	

Analysis showed that the reason for the low score at the thigh was that the rigidity coefficient of the material at the headlight was considerably large. The result was the absorption of kinetic energy at the thigh collision being lower than that of the other parts. This outcome generated a different acceleration with other parts, forming a velocity difference and generating a markedly large bending moment.

IMPROVEMENT ANALYSIS

Energy Changes

The kinetic energy of the pedestrian's legs during the collision is as follows:

$$E = \frac{1}{2}MV^2, \tag{1}$$

The front-end structure of the vehicle absorbs energy as follows:

$$W = \int_{\Delta x} f dx = F \cdot \Delta x \cdot \eta, \tag{2}$$

Energy is satisfied during impact as follows:

$$\frac{1}{2}MV^2 = F \cdot \Delta x \cdot \eta, \tag{3}$$

Joint equations (1) to (3) can be obtained as follows:

$$a = \frac{0.5V^2}{\Delta x \cdot \eta}, \tag{4}$$

Where: M is the mass of the lower limb impactor; V is the velocity of the impactor movement; Δx is the intrusion of the lower limb impactor into the front-end structure of the car; F is the force between the front-end structure of the car and the leg impactor and $F=Ma$; η is the energy absorption rate; and a is the acceleration of the leg.

The results showed an excessive bending moment because the kinetic energy absorbed at the impact between the thigh and the headlight was lower than that of the other parts, which made the thigh produced a larger acceleration. To reduce the acceleration of the leg at the headlight, transferring part of the kinetic energy to the headlight in the collision can be considered:

$$\frac{1}{2}MV^2 = F \cdot \Delta x \cdot \eta + \frac{1}{2}mv^2, \tag{5}$$

At this point, the leg acceleration a can be deduced as follows:

$$a = \frac{0.5V^2}{\Delta x \cdot \eta}\left(V^2 - \frac{m}{M}v^2\right), \tag{6}$$

where m is the mass of the headlight and v is the speed of headlight movement.

Equation (6) indicates that the leg acceleration is reduced after part of the kinetic energy is transferred to the headlight. Therefore, this study considers the study of headlight structural parameters to improve pedestrian leg safety.

Structural Parameter Study

The process of structural parameter study is to expand the headlight backward space without changing the initial position of the headlight. The moment of collision of the thigh with the headlight transfers part of the kinetic energy to the headlight. The headlight gains kinetic energy and moves backward, being blocked by the headlight rear baffle. The thigh continues to collide with the more effective part of the front bumper, which deforms and absorbs energy. The thigh continues to move forward and eventually collides with the headlight again. An additional kinetic energy absorption process exists in this solution compared with the solution where the headlights are directly moved back. The first impact of the thigh with the headlight does not cause the thigh to generate a large reverse velocity. The reason is that the headlight is not fixed in the direction of the impact and does not generate a large bending moment as it generally does before the optimization.

The structural parametric study is required to determine the exact length of the headlight setback space but does not require a specific design of the headlight structure. The headlight setback space should not be considerably long, considering the structural requirements of other parts of the vehicle. This study is attempted at 5-mm intervals. Accordingly, determining the appropriate headlight moving space needs repeating the test. The specific steps are as follows (Fig. 9).

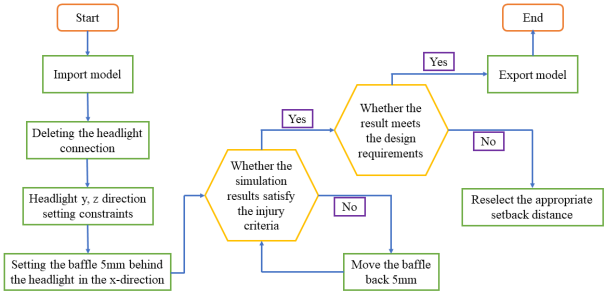

Fig. 9. Structural parameters study process.

(1) The connection between the headlights and the rest of the car model is deleted.

(2) Constraints on the original connection are set, headlights' lateral (y) and vertical (z) translations and rotations are limited, and the motion of the vehicle's traveling direction (x) are not limited.

(3) On the basis of engineering experience, a baffle is created 5 mm behind the headlight along the collision direction.

(4) The model is exported and LS-DYNA is used for calculation. The calculation results is exported and checked whether or not they meet the evaluation index. If the standard is not met, then the baffle of the limit headlight movement is moved back by 5 mm to increase the setback space. Thereafter, the calculation is submitted again until the final calculation result meets the evaluation index.

(5) The headlight displacement space is

checked if it meets the design requirements. If not, then the setback space is selected again and the calculation is started again as well.

Improved Results

When the headlight setback space reached 40 mm, the Femur_up bending moment was 331 Nm, the Femur_mid bending moment was 382 Nm, and the Femur_low bending moment was 337 Nm. All were lower than the specified high-performance limits (Fig. 10). Where the Femur_mid appeared the maximum bending moment of the entire thigh area, which was reduced by 73 Nm compared to the results of the initial scheme (Fig. 11). At this point, the safety score of the improved scheme also reached the full mark.

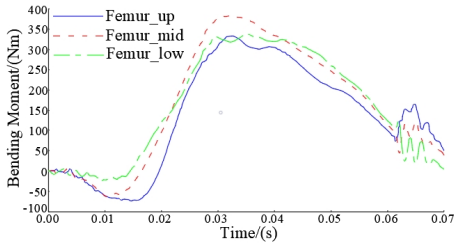

Fig. 10. Variation curve of thigh bending moment after optimization.

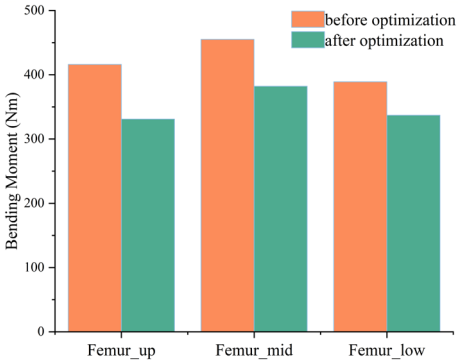

Fig. 11. Comparison of thigh bending moment values.

The analysis of the variation of the thigh bending moment showed that in the 0–20 ms stage, the pedestrian's knee first collided with the front bumper skin. At this time, the thigh did not collide with the headlight, and the direction of the bending moment was opposite to the set direction, and thus was negative. At 20 ms, the thigh collided with the headlight. Given the presence of a set setback space at the headlight, there was no blockage when the thigh collided with the headlight, and the thigh continued to maintain its previous motion. At this time, the increasing trend of the bending moment curve did not change significantly. At about 30 ms after impact, the rear end of the headlight moved to the fender. The headlight collided with the thighs again and the thigh bending moment reached the maximum value. Thereafter, the thigh gained velocity in the opposite direction and started to move backward. The displacement difference between each marker point at the thigh and knee decreased, and the bending moment decreased accordingly. After reaching 60 ms, contact between aPLI and the car ended, the thigh and calf kept swinging in the air, and the bending moment change was no longer regular.

Future study

In this study, pedestrian leg injuries are reduced by improving the structural parameters of headlights. The results and the research process can provide ideas for the design of headlights, which can guide future vehicle safety assessment and design. Meanwhile the current study has limitations. Firstly, only one specific working condition and a specific SUV model are used. Although they are representative, different models and more application scenarios can be considered in subsequent studies. Second, the study applies a-PLI and focuses only on the lower limb response of pedestrians. In actual collisions, pedestrians' heads and chests will also suffer serious injuries. Therefore, we can consider applying human body finite element model to study the effects of SUVs on pedestrians' injuries in various body parts.

CONCLUSIONS

This study establishes the car and pedestrian lower limb impact conditions. Lower limb injuries are analyzed and shortcomings in pedestrian lower limb impact safety are identified. By analyzing the lower limb energy changes during the collision process and studying the headlight space structural parameters, the safety of the pedestrian lower limb is finally improved. This study provides a reference for automobile structural design and pedestrian lower limb protection. The following conclusions are obtained.

(1) The hardness of the material used at the headlight is considerably larger than that of the other parts, such as the front bumper skin. The energy absorption effect is poor, and the thigh and other parts of the thigh will produce a markedly large speed difference. The result is a significantly large bending moment.

(2) When pedestrians collide with the headlight part of the car, the headlight is shifted back, which can reduce the kinetic energy of the thigh during the impact. Consequently, the bending moment of the thigh is reduced, thereby achieving the purpose of pedestrian protection.

REFERENCES

Aekbote, K., Schuster, P.J., Kankanala, S.V., Sundararajan, S., and Rouhana, S.W., "The biomechanical aspects of pedestrian

protection," *INT J VEHICLE DES*, Vol. 32, No. 1-2, pp. 28-52 (2003).

Altai, Z., Viceconti, M., Offiah, A.C., and Li, X., "Investigating the mechanical response of paediatric bone under bending and torsion using finite element analysis," *Biomech. Model. Mechanobiol*, Vol. 17, pp. 1001-1009 (2018).

Bhagat, M., Chalipat, S., and Ranade, A., "Influence of vehicle front end design on pedestrian lower leg performance for SUV class vehicle," *SAE International Journal of Passenger Cars-Mechanical Systems*, No. 4, pp. 12-21 (2011).

Carter, E.L., Neal-Sturgess, C.E., and Hardy, R.N., "APROSYS in-depth database of serious pedestrian and cyclist impacts with vehicles,"*Int. J. Crashworthiness*, Vol. 13, No. 6, pp. 629-642 (2008).

Cao, G.Y., Wang, Y., Wang, M., Lu, L., and Wang, P.X., "Research on aPLl Leg Type of Pedestrian Protection," *Auto Time*, No. 02, pp. 155-158 (2024).

Cheng, R., Pan, Y., and Xie, L., "Analysis of vehicle-pedestrian accident risk based on simulation experiments," *MATH PROBL ENG*, (2022).

Chen, L., Liu, H.D., Yu, C.C., Lou, Z.Y., and Zhang, H.Y., "Application and vehicle development of pedestrian protection advanced pedestrian legform impactor (aPLI)," *Automotive Technology*, No. 3, pp. 8-13 (2021).

Chen, P., and Yang, K.T., "Research on dynamic calibration method of aPLI impactor," *Auto Time*, No. 08, pp. 188-190 (2021).

China Automotive Technology and Research Center Co. Ltd (CATARC), "C-NCAP Management Rules (2024 edition)," (2024).

Fu, Y., Xu, H., Lin, G., Zhan, Z., Wang, P., Chen, R., and Yu, H., "A Design and Optimization Method for Pedestrian Lower Extremity Injury Analysis with the aPLI Model," *SAE Technical Paper*, No. 2020-01-0929 (2020).

Hou, S., Luo, K., Xie, B., and Wu, C.P., "Study on the Enhancement of the Crash Performance of aPLI Legform in a Vehicle Model," *Automotive Engineering*, Vol. 42, No. 11, pp. 1558-1565 (2020).

Hou, S., Wu, Z.Q., and Luo, K., "Multi-objective Optimization of aPLI Impact Performance of a SUV," *SAECCE 2022*, pp.155-160 (2022).

Hu, W., Monfort, S. S., and Cicchino, J. B., "The association between passenger-vehicle front-end profiles and pedestrian injury severity in motor vehicle crashes," *J. Saf. Res*, No. 90, pp. 115-127 (2024).

Isshiki, T., Konosu, A., and Takahashi, Y., "Development and evaluation of the advanced pedestrian legform impactor prototype which can be applicable to all types of vehicles regardless of bumper height-Part 1: finite element model," *IRCOBI* (2016).

Long, Y.C., Hao, H.Z., Li, F., and Fei, J., "Biofidelity of current legform impactor in pedestrian safety test," *Automotive Safety and Energy*, Vol. 12, No. 4, pp. 475-482 (2021).

Matsui, Y., Doi, T., Oikawa, S., and Ando, K., "Features of fatal pedestrian injuries in vehicle-to-pedestrian accidents in Japan," *SAE INT J TRANSP SAF*, Vol. 1, No. 2, pp. 297-308 (2013).

Mo, F., Duan, S., Jiang, X., Xiao, S., Xiao, Z., Shi, W., and Wei, K., "Investigation of occupant lower extremity injures under various overlap frontal crashes," *Int. J. Automot*, Vol. 19, pp. 301-312 (2018).

Mo, F., Jiang, X., Duan, S., Xiao, Z., Xiao, S., and Shi, W., "Parametric analysis of occupant ankle and tibia injuries in frontal impact," *Plos one*, Vol. 12, No. 9, pp. e0184521 (2017).

Tyndall, J., "The effect of front-end vehicle height on pedestrian death risk," *Econ.*, No. 37, pp. 100342 (2024).

Wang, B., Wang, F., Otte, D., Han, Y., and Peng, Q., "Effects of passenger car front profile and human factors on pedestrian lower extremity injury risk using German in-depth accident data," *Int. J. Crashworthiness*, Vol. 24, No. 2, pp. 163-170 (2019).

Wei, Z.S., Huang, H.P., Cao, G.Y., and Yan, D.D., "Base on New Leg APLl in A-Class Car Application," *Automotive Engineer*, No. 10, pp. 42-45 (2021).

Xu, F.H., Yang, Q.K., Wu, Z.X., and Yan, G.F., "Study on aPLI legform of pedestrian protection based on a SUV," *Environmental Technology*, No. S1, pp. 54-58 (2021).

You, S.Q., Xiao, S., Chen, W., Tian, T.F., Zhao, X.L., and Zhang, H., "Investigation of Ankle Joint Responses with Emergency Braking During Frontal Impact," *J CHIN SOC MECH ENG*, Vol. 53, No. 5, pp. 441-451 (2022).